Evidence for $M1$ strength in the $^3H(\vec{p},\gamma)^4He$ reaction

D. J. Wagenaar,* N. R. Roberson, and H. R. Weller
Duke University and Triangle Universities Nuclear Laboratory, Duke Station, Durham, North Carolina 27706

D. R. Tilley
North Carolina State University, Raleigh, North Carolina 27695
and Triangle Universities Nuclear Laboratory, Duke Station, Durham, North Carolina 27706

(Received 13 September 1988)

Angular distributions of cross sections and analyzing powers were measured for the $^3H(\vec{p},\gamma)^4He$ reaction at incident proton energies of 2.0, 5.0, and 9.0 MeV. The 90° analyzing power was measured at 11 energies between 0.8 and 9.0 MeV. A transition matrix element analysis indicated that the inclusion of $M1$ strength gave better fits and eliminated the anomalously large $^3D_2$ ($E2$) strength reported in earlier work. An $E1$-plus-$E2$ direct capture calculation was performed. It is shown that this calculation can be brought into agreement with the data if an $M1$ strength comparable to that found in the T-matrix element analysis (0.5–1.0% of the total capture cross section) is added.

I. INTRODUCTION

Previous work on the $^3H(\vec{p},\gamma)^4He$ reaction has consisted of measurements of angular distributions of analyzing powers and cross sections at incident proton energies from 6 to 16 MeV.[1] These data were analyzed in terms of $E1$ and $E2$ transition matrix elements. The results indicated an anomalously large $^3D_2(E2)$ capture amplitude (notation $^{2S+1}L_J$) which accounted for as much as 50% of the total $E2$ cross section, in contradiction to expectations and calculations.[2] Further study indicated that this $\Delta S=1$ $E2$ strength could be reduced by including $E3$ radiation in the analysis, although the amount of $E3$ strength required was much larger than that predicted by a direct capture model calculation.[3]

In the present work, measurements of angular distributions of cross sections and analyzing powers for the $^3H(\vec{p},\gamma)^4He$ reaction were extended to lower energies. Data were obtained at incident proton energies of 2.0 and 5.0 MeV. In addition, the 90° analyzing power was measured at eleven proton bombarding energies ranging from 0.8 to 9.0 MeV. These data, along with previous accurate data obtained at $E_p=9.0$ MeV,[3] were analyzed in an attempt to arrive at a result which gave a physically reasonable $\Delta S=1$ $E2$ strength ($^3D_2$). The analysis was expanded to include $M2$, $E3$, or $M1$ radiation in addition to the $E1+E2$ strength. It was found that acceptable fits could be found at all energies for which angular distribution data existed only when $M1$ strength was included in the analysis along with $E1$ and $E2$ terms.

A direct $E1+E2$ capture calculation was also performed for this reaction up to $E_p=9.0$ MeV. Good agreement was achieved with all experimentally determined angular distribution coefficients except b_1. However, when $M1$ strength comparable to that found in the $E1$-$E2$-$M1$ T-matrix analysis was added to the results of this $E1+E2$ calculation, good agreement with the b_1 coefficient and the analyzing power at 90° was observed. These results indicate that $M1$ strengths of 0.5–1.0 % of the total cross section are present in the $^3H(p,\gamma)^4He$ reaction at bombarding energies below 9.0 MeV.

II. EXPERIMENTAL DETAILS

A fairly complete description of the TUNL capture setup has been published elsewhere;[4] only the details relevant to the present work will be discussed here.

The polarized proton beams used in the measurements were produced by the TUNL Lamb-shift polarized ion source. Polarized proton beams of 100–150 nA were available on target. Beam polarizations were measured via the quench ratio method[5] with typical values of 0.7 ± 0.03. These results were checked by measuring the analyzing powers of elastically scattered 9.4 MeV protons from tritium and using previous results[6] to deduce the beam polarization. The two results were found to agree within error ($\pm3\%$).

The tritium targets used in this work were in the form of 5 μm thick tritiated titanium foils. Six different such foils were used during the course of the experiment. The target thicknesses were determined by measurements of the yields of elastically scattered protons at previously measured energies.[7–9] The six targets of the present experiment were found to have tritium mass thicknesses which ranged from 60–110 $\mu g/cm^2$. Titanium foils containing no tritium were used to generate background spectra. These foils were of the same thickness as the actual target foils.

Our two anticoincidence shielded 25×25 cm NaI(Tl) spectrometers were used to detect the capture γ rays from the $^3H(p,\gamma)^4He$ reaction. These detectors were used in a variety of geometries. For example, analyzing powers were obtained with the two detectors positioned symmetrically on the left- and right-hand sides of the beam line. This arrangement eliminates many potential sources of systematic error, such as inaccurate beam

current integration or variations in the target thickness. Furthermore, geometrical and count rate requirements led to the use of different target-to-detector distances while background rates led to different thicknesses of paraffin being placed in front of the detector. A summary of the experimental conditions is presented in Table I.

The low-energy polarized proton beams desired for this experiment could not be produced directly with the TUNL FN-tandem accelerator due to poor beam transmission at very low terminal potentials. Incident proton energies of $E_p < 2.5$ MeV on target were therefore obtained by the use of degrading foils. Three Havar foils, each having a thickness of 6.35 μm, were used to provide polarized proton beams in the energy range of 0.8–2.0 MeV.

Measurements were performed in order to determine the effect of these foils on the energy, energy spread, and polarization of the beam at the target. The actual energy and energy spread were measured by use of a thin (5 $\mu g/cm^2$) carbon target. Elastically scattered protons were detected with and without the Havar foils in the way of the beam. For example, an incident proton beam of 3.2 MeV was found to have an energy of 2.00±0.05 MeV and an energy spread of 135 keV after passing through the Havar foils. The angle straggling of the beam due to the Havar foils was calculated using the expressions of Ref. 10. Recent measurements[11] have shown that at our energies these calculated values are slightly larger than the measured ones. A calculated value of $\theta_{1/e}$ of 6.7° was obtained for 2.5 MeV protons incident on three 6.35 μm layers of Havar.

Basic considerations regarding the time which the protons spend in traversing the Havar foils compared to the Larmor period of the ground state of hydrogen indicate that depolarization effects of the Havar foils should be small. In order to verify this the depolarization was measured using the $^4He(\vec{p},p)^4He$ reaction. This was done by measuring the analyzing power produced by a direct 2.0 MeV beam (of low intensity) and then repeating the measurement with a 3.2 MeV incident beam degraded to 2.0 MeV by means of the Havar foils. The result gave a ratio for the former to the latter analyzing power of 0.97±0.05. It can be concluded that the depolarization in the Havar foil is not significant to within the accuracy of the present experimental measurements of analyzing powers.

Backgrounds due to cosmic rays and to the beam interacting with everything except the tritium were measured and subtracted from the data. The cosmic ray background under the γ ray peaks was determined by summing a region of the spectrum corresponding to higher energies and using the energy dependence of the beam off spectrum to extrapolate to the peak region. Although essentially all of the background at $E_p = 9.0$ MeV was due to cosmic-rays, noncosmic background was present at the lower energies, especially at extreme angles. In these cases spectra were taken with the untritiated foils and used to make background corrections. These corrections were typically ~2%, although at $\theta_{lab} = 20°$ the correction rose to 7% of the true events.

III. DATA AND ANALYSIS

Angular distributions of cross section were obtained at $Ep = 2.0$, 5.0, and 9.0 MeV. The measurements were made with an unpolarized beam having an intensity sufficient to allow the 2.0 MeV measurements to be performed without the use of degrading foils. The measurements at the various angles were normalized by means of

TABLE I. NaI (Tl) detector operating parameters. Upper values are those used with polarized beams; lower values with unpolarized.

Proton energy[a] (MeV)	θ_{lab} (deg)	Detector distance[b] (cm)	Paraffin thickness[c] (cm)	Detector[d]
0.82,1.45	90	39.1	0	Both[f]
2.0	70,90	58.4	0	Both
2.0	50,110	80.6	0	Both
2.0	30,130,148.5	123.8	5.1	Both
3.0–9.0	90	55.9	20.3	Both
5.0	45–134	84.4	20.3	Both
5.0	140,148.5	123.8	20.3	Right
5.0	27.5	129.1	20.3	Left
5.0	20	148.1	20.3	Left
9.0	31–140	123.8	20.3	Both
2.0,5.0	20–155	129.1	20.3	Left
2.0,5.0	90	80.6	20.3	Right[e]
9.0	30–150	123.8	20.3	Both
9.0	80	80.6	20.3	Left[e]

[a]Incident on target.
[b]To front face of NaI (Tl) crystal.
[c]In front of collimator.
[d]With respect to beam direction.
[e]When used as γ ray monitor.
[f]"Both" designates detectors both right and left of beam direction.

TABLE II. Experimental a_k and b_k coefficients. Errors shown are the statistical uncertainties.

E_p (MeV)	2.0	5.0	9.0
a_1	0.069±0.005	0.135±0.005	0.223±0.003
a_2	−0.981±0.005	−0.970±0.005	−0.966±0.004
a_3	−0.060±0.009	−0.150±0.009	−0.238±0.007
a_4	−0.011±0.010	−0.020±0.009	−0.008±0.009
χ^2	0.883	0.833	1.78
b_1	−0.013±0.003	−0.008±0.003	−0.004±0.005
b_2	0.003±0.002	0.058±0.002	0.062±0.003
b_3	0.000±0.001	0.003±0.001	0.008±0.002
b_4	0.002±0.001	0.000±0.001	0.002±0.003
χ^2	0.321	0.525	0.284

a solid state charged particle detector which observed the elastically scattered protons from tritium.

The angular distribution at each energy was fit by a Legendre polynomial expansion, i.e.,

$$\sigma(\theta)=A_0\left[1+\sum_{k=1}^{4} a_k Q_k P_k(\cos\theta)\right] .$$

The Q_k coefficients correct for the finite size of the detectors. Excellent χ^2 values were found when $k=1-4$ terms were included. The resulting a_k coefficients are shown in Table II. The data and the polynomial fits are presented in Fig. 1.

An angular distribution of the analyzing power was obtained at $E_p=2.0$ MeV using the degrading foils. These data were relatively difficult to obtain due to the decreased cross section and the reduced analyzing power at this energy. Angular distributions of the product of cross section times analyzing power are also shown in Fig. 1. In this case the data were fit by an associated Legendre polynomial expansion

$$\frac{\sigma(\theta)A(\theta)}{A_0}=\sum_{k=1}^{4} b_k Q_k P_k^1(\theta) .$$

Again, the Q_k factors take the finite size of the NaI detector into account. The resulting b_k coefficients are presented in Table II along with the a_k coefficients.

In addition to these angular distribution data, the analyzing power at 90° was measured at 11 energies between 0.8 and 9.0 MeV. The results are plotted in Fig. 2

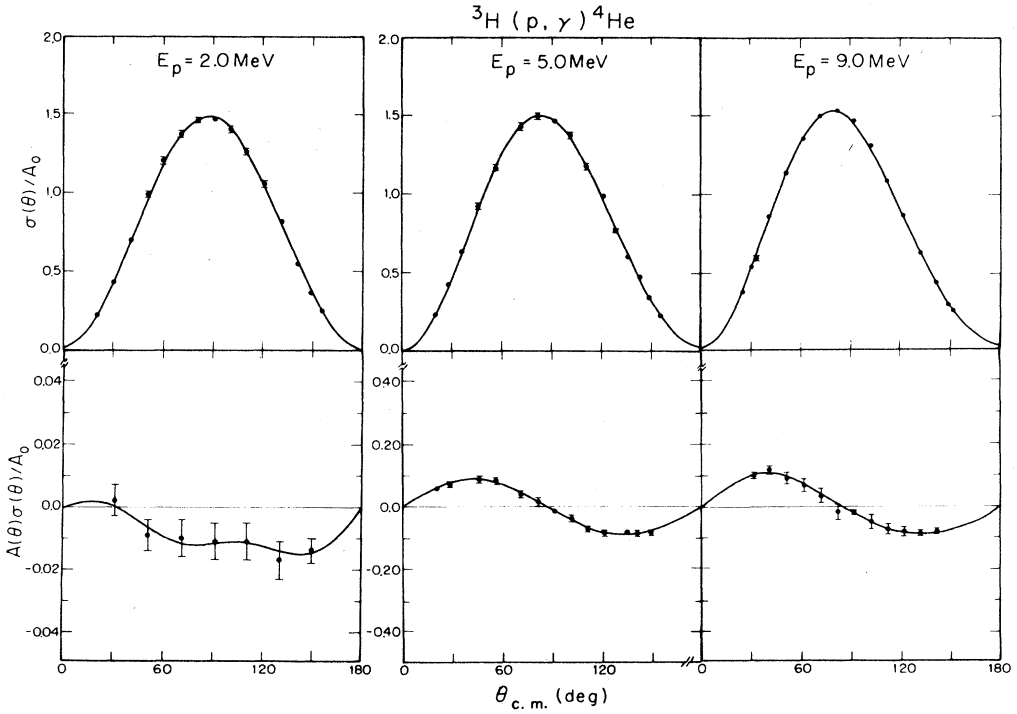

FIG. 1. Angular distributions of cross sections and analyzing powers for $E_p=2.0$, 5.0, and 9.0 MeV. The solid lines represent the Legendre and associated Legendre polynomial fits to the data. Error bars represent the statistical uncertainties associated with the data.

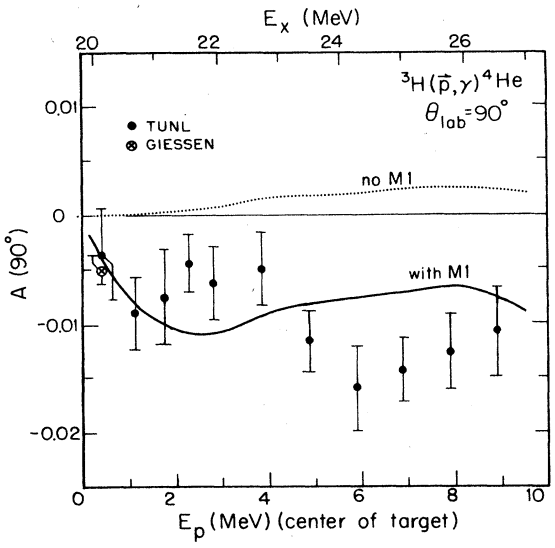

FIG. 2. The analyzing powers at 90° ($A(90°)$) of the present work (TUNL) as a function of proton beam energy (lab). The dotted line is the result of the direct capture calculation ($E1+E2$ only); the solid line is the result of adding $^3S_1M1$ strength (see text) to this calculation.

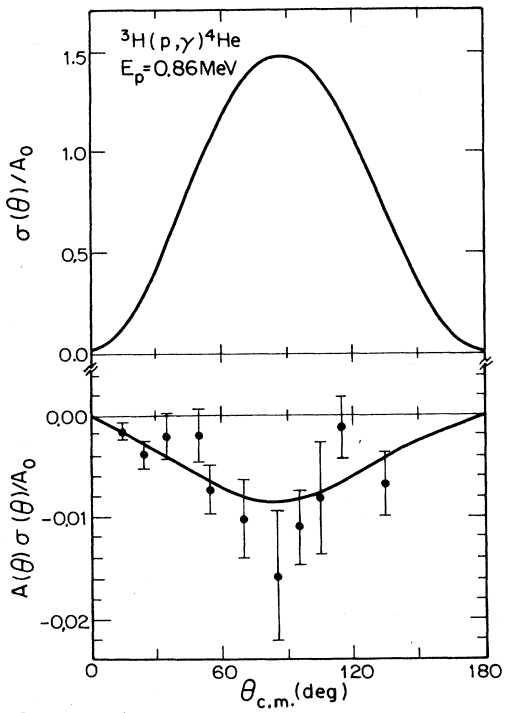

FIG. 3. Data shown here were obtained by combining the data of Ref. 12 with extrapolated a_k coefficients. The solid line for $\sigma(\theta)/A_0$ is the result of this extrapolation. The line for $A(\theta)\sigma(\theta)/A_0$ is the result of fitting in terms of associated Legendre polynomials.

as a function of center-of-target energy. The three points below 2.0 MeV were taken using Havar foils to lower the beam energy. The initial proton beam energies were 2.0, 2.87, and 3.2 MeV. The energies of the protons on target were measured by scattering from a thin carbon target and were found to be 0.8, 1.4, and 2.0 MeV, respectively. The center-of-target energies were calculated to be 0.4, 1.14, and 1.76 MeV.

In addition to the data reported here, a measurement of the vector analyzing powers for the $^3H(p,\gamma)^4He$ reaction at low energies ($E_p=0.86$ MeV) has been previously reported.[12] In order to construct a cross section $\sigma(\theta)$ at this energy, we extrapolated the values of the a_k coefficients obtained in the present work. The resulting $\sigma(\theta)$ and $\sigma(\theta)A(\theta)$ curves are shown in Fig. 3. The extrapolated a_k coefficients and the b_k coefficients obtained from fitting the $\sigma(\theta)A(\theta)$ data are

$$a_1=0.056,\quad b_1=-0.008\pm0.001\ ,$$
$$a_2=-0.992,\quad b_2=-0.001\pm0.001\ ,$$
$$a_3=-0.053,\quad b_3=0.000\pm0.001\ ,$$
$$a_4=-0.003,\quad b_4=0.000\pm0.001\ .$$

Additional measurements of the $^3H(\vec{p},\gamma)^4He$ reaction in this energy range have been reported by the Stanford[1] and the Ohio State University (OSU) groups.[13] The a_k and b_k coefficients of the present work are shown along with these previous results in Figs. 4 and 5, respectively.

Previous analyses of the $^3H(\vec{p},\gamma)^4He$ data have extracted the transition matrix elements from the measured a_k and b_k coefficients. When a pure $E1$-$E2$ analysis was performed at $E_p=9$ MeV, a triplet $E2$ strength was obtained which was considerably larger than that predicted by both the recoil corrected continuum shell model (RCCSM) and direct capture model calculations.[1,3] It has been suggested that this result may be due to the neglect of $M2$,[14] or $E3$ (Ref. 3) radiation in the T-matrix analysis.

Both a RCCSM calculation[14] and a direct-capture

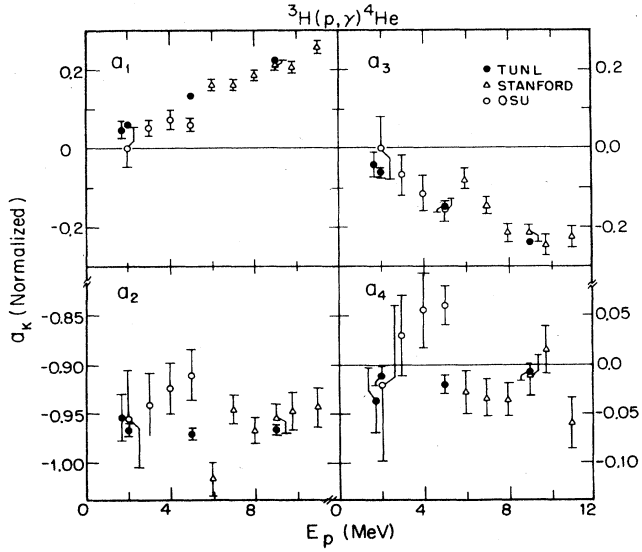

FIG. 4. The a_k coefficients of the present work (TUNL) along with those of Ref. 1 (Stanford) and Ref. 13 (OSU).

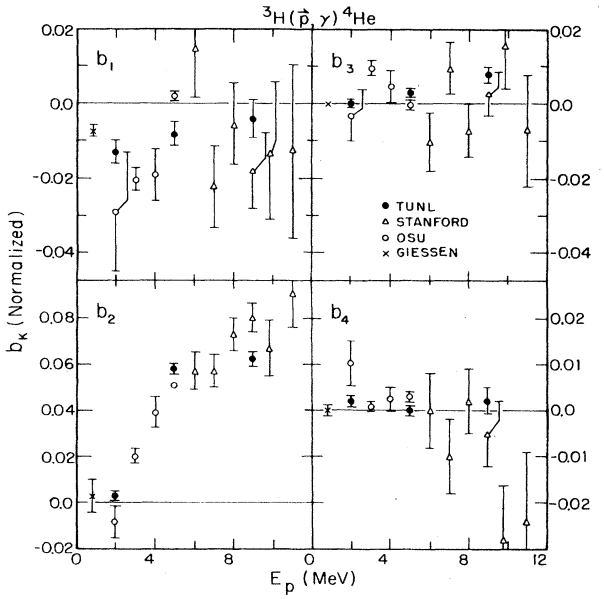

FIG. 5. The b_k coefficients of the present work (TUNL) along with those of Ref. 1 (Stanford), Ref. 13 (OSU), and Ref. 12 (Giessen).

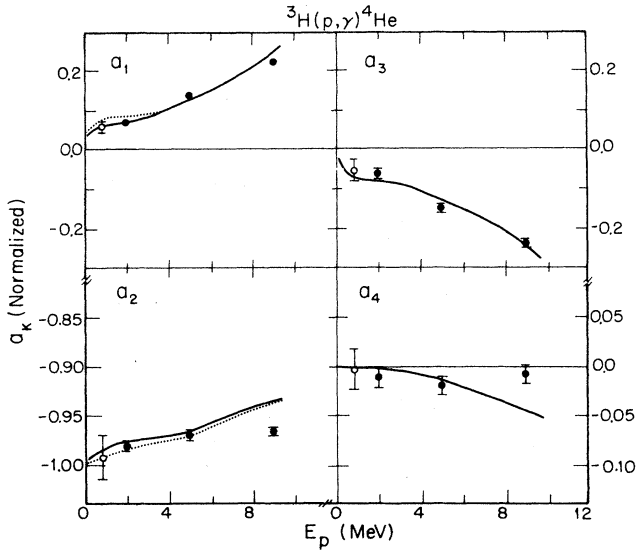

FIG. 6. The present a_k coefficients (solid dots) plus the extrapolated low E value (open circle). The dotted line is the result of the $E1$-plus-$E2$ direct capture calculation. The solid line is the result of adding $M1$ to this calculation.

model calculation predict that the magnitudes of b_1 and b_3 should increase smoothly from zero with increasing energy if only $E1$ and $E2$ contributions are considered. As can be seen in Fig. 5, this behavior is not observed experimentally. It therefore seems necessary to include one or more additional multipoles in the T-matrix analysis.

A. *E1-E2-M2* analysis

In this case the $E1$-$E2$ analysis was extended to include the two possible $M2$ elements, $^3P_2$ and $^3F_2$ (notation $^{2S+1}L_J$ denotes the quantum numbers of the scattering state). Each $M2$ element was separately included with the $E1$ and $E2$ elements in the T-matrix analysis at all four energies (0.86, 2.0, 5.0, and 9.0 MeV). The case with both elements included together was also considered. No satisfactory solution was obtained for any case of the four energies. The failures had large reduced χ^2, unphysically large $^3D_2$ amplitudes, and/or no minimum χ^2 value.

B. *E1-E2-E3* analysis

In this case the $^1F_3$ and $^3F_3$ ($E3$) elements were included in the T-matrix analysis. As discussed in a previous paper,[3] this analysis can lower the $^3D_2$ amplitude to a value consistent with model predictions, but an $E3$ amplitude ($^1F_3$) which is three orders of magnitude larger than the value predicted by direct capture model is required to do this.[3]

C. *E1-E2-M1* analysis

In this case the T-matrix analysis was extended to include the $^3S_1$ and $^3D_1$ $M1$ matrix elements. As before, both $M1$ matrix elements were included along with the $E1$ and $E2$ ones in a T-matrix element analysis at the four energies.

The results indicated that the $^3S_1(M1)$ term produced better fits at all the energies than the $^3D_1(M1)$ term did.

TABLE III. $E1$-$E2$-$M1$ transition matrix amplitudes and phases for ^{3}H($\vec{p}$,γ)^{4}He reaction. The amplitudes are given as a percentage of the total cross section, the phases are given relative to $\Phi(^1P_1)=0$. The $^3D_2$ amplitude was set to equal zero here.

E_p(lab) (MeV)		0.86	2.0	5.0	9.0
Amp	Phase (deg)				
$^1P_1$		98.6±0.8	98.3±0.6	97.9±0.6	97.6±0.4
	$\Phi(^1P_1)$	0.0	0.0	0.0	0.0
$^3P_1$		0.1±0.2	0.02±0.04	1.1±0.7	1.3±0.3
	$\Phi(^3P_1)$	191±35	213±70	51±19	56±12
$^1D_2$		0.2±0.5	0.4±0.5	0.3±0.1	0.9±0.2
	$\Phi(^1D_2)$	64±34	68±14	17±30	−18±16
$^3S_1$		1.1±1.1	1.2±0.8	0.7±1.0	0.3±0.4
	$\Phi(^3S_1)$	2±1	4±2	1±4	6±9
	χ^2	0.73	0.89	0.81	1.4

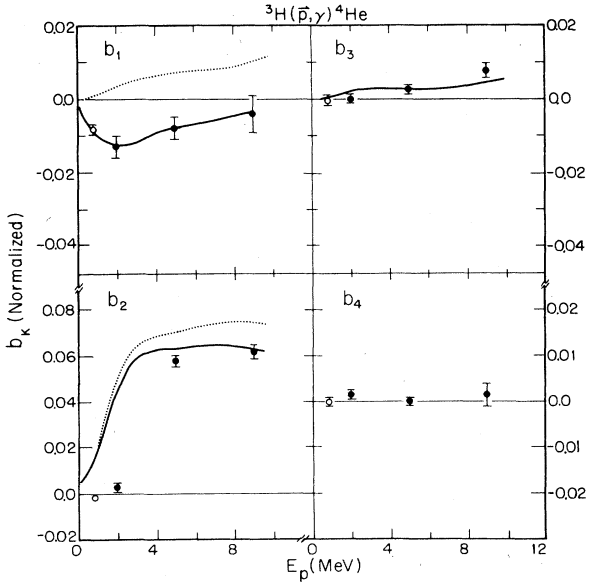

FIG. 7. Same as Fig. 6 but for b_k. The open circle data point was obtained using the data of Ref. 12 as discussed in the text.

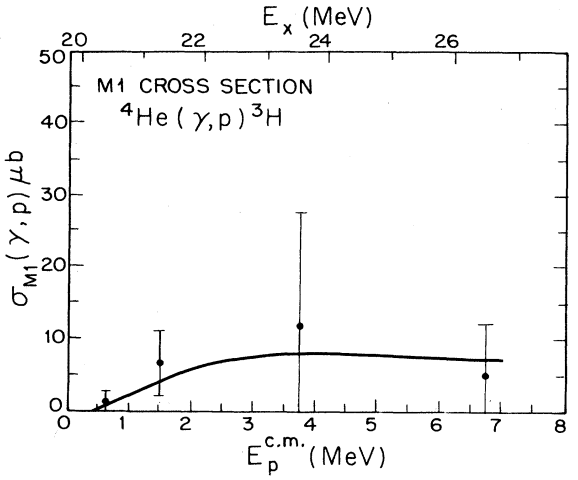

FIG. 8. The data points represent $M1$ cross sections determined from the $E1$-$E2$-$M1$ T-matrix analysis (Table III). The solid line represents the $M1$ cross section added to the $E1$-$E2$ direct capture calculation in order to fit b_1 (Fig. 7) and $A(90°)$ (Fig. 2).

It was also found that $E2$ radiation is present even at the lowest energy. Good fits could be obtained with the $^3D_2E2$ strength set equal to zero. The results of this analysis are summarized in Table III.

IV. DIRECT CAPTURE CALCULATIONS

The results of the previously described T-matrix analyses suggest that the difficulty with previous analyses of the $^3H(\vec{p},\gamma)^4He$ reaction was the neglect of the $^3S_1(M1)$ transition matrix element. In order to pursue this further a direct capture model calculation was performed.[15] The bound state wavefunction was computed by adjusting the well depth of a Woods-Saxon potential to obtain the correct ^4He binding energy for the $p+T$ channel. An optical model potential was used to generate the scattering state wavefunctions. The optical model parameters were taken from Ref. 16, with the spin-orbit strength reduced by 20% (to produce better fits to the b_2 coefficient). The electric operators were taken to have the form given by the long-wavelength approximation (r^L). The calculations were performed with $E1$ and $E2$ included. The results were compared to the measured a_k and b_k coefficients of the present work in Figs. 6 and 7. It can be seen here that this model rather successfully reproduces the measured coefficients, except for the case of b_1. If $M1$ radiation is added it will have a relatively large effect on b_1 (via $E1$-$M1$ interference) with small or zero effects on b_2, b_3, and b_4.

Since it is difficult or impossible to make a reliable direct capture calculation of the $M1$ amplitudes, we attempted to add $M1$ strength to the calculated $E1+E2$ strength to reproduce the b_1 data. Based on the results of the T-matrix analysis, we assumed that only the $^3S_1(M1)$ term was present. The relative phase angle (relative to the $^1P_1$ term) of this term was allowed to vary from 0° to 180° in the fitting procedure. The result of this fitting indicated that reasonable results could be obtained for relative phase angles of 0°–5°, in good agreement with the 3° result of our T-matrix analysis. With the phase set at 3°, the $^3S_1$ strength needed to fit the b_1 coefficients peaked at 0.9% of the total cross section at 2.0 MeV and fell to 0.4% at 9.0 MeV. The results are shown in Figs. 6 and 7.

The analyzing power at 90° ($A(90°)$) is an observable which is particularly sensitive to the size of the $E1$-$E2$ and $E1$-$M1$ interference terms—much like b_1. The results of our direct capture calculation both with and without the previously determined $M1$ strength included are shown in Fig. 2 along with the data. Clearly the measured analyzing powers at 90° support the need to include $M1$ radiation. The data above 5.0 MeV do, in fact, suggest the possibility of additional energy dependent structure in the $M1$ strength.

The $M1$ cross sections obtained in our T-matrix element analysis (Table III) were converted to $^4He(\gamma,p)^3H$ cross sections and are plotted in Fig. 8. The solid curve shown here represents the $M1$ cross sections which were added to the direct-capture model calculation in order to fit the b_1 coefficients. The presence of this $M1$ strength is supported by the $A(90°)$ data of Fig. 2. Its existence also eliminates the need for any $^3D_2(E2)$ strength, which is consistent with predictions of both the present direct-capture calculations and the RCCSM model calculations of Ref. 14.

This work was supported by the U.S. Department of Energy, Office of High Energy and Nuclear Physics, under Contract No. DE-AC05-76ER01067.

*Present address: University of North Carolina at Chapel Hill, Chapel Hill, NC 27511.

[1]G. King, Ph.D. thesis, Stanford University, 1978; see also Ref. 2 below.

[2]D. Halderson and R. J. Philpott, Nucl. Phys. **A359**, 365 (1981).

[3]D. J. Wagenaar, N. R. Roberson, H. R. Weller, and D. R. Tilley, Phys. Rev. C **32**, 2155 (1985).

[4]H. R. Weller and N. R. Roberson, IEEE Trans. Nucl. Sci. **NS-28**, 1268 (1981).

[5]T. A. Trainor, T. B. Clegg, and P. W. Lisowski, Nucl. Phys. **A220**, 533 (1974).

[6]R. A. Hardekopf, P. W. Lisowski, T. C. Rhea, R. L. Walter, and T. B. Clegg, Nucl. Phys. **A191**, 481 (1972).

[7]J. E. Brolley, Jr., T. M. Putnam, L. Rosen, and L. Stewart, Phys. Rev. **117**, 1307 (1960).

[8]G. M. Hale and R. K. Umerjee, Nucl. Phys. **A156**, 570 (1970).

[9]R. Kankowsky, J. C. Fritz, K. Kilian, A. Neufert, and D. Fick, Nucl. Phys. **A263**, 29 (1976).

[10]J. B. Marion and B. A. Zimmerman, Nucl. Instrum. Methods **51**, 93 (1967).

[11]D. R. Dixon, G. L. Jensen, S. M. Morrill, C. J. Connors, R. L. Walter, C. R. Gould, and P. M. Thambiduria, IEEE Trans. Nucl. Sci. **NS-28**, No. 2, 1295 (1981).

[12]D. Krämer, W. Arnold, H. Berg, and G. Clausnitzer, in *Polarization Phenomena in Nuclear Physics—1980 (Fifth International Symposium, Santa Fe),* Proceedings of the Fifth International Symposium on Polarization Phenomena in Nuclear Physics, AIP Conf. Proc. No. 69, edited by G. G. Ohlson, R. E. Brown, N. Jarmie, W. W. McNaughton, and G. M. Hale (AIP, New York, 1981), Part 2, p. 1258.

[13]M. A. Kovash, Ph.D. dissertation, The Ohio State University, 1979.

[14]D. Halderson and R. J. Philpott, Nucl. Phys. **A359**, 365 (1981).

[15]C. Rolfs, Nucl. Phys. **A217**, 29 (1973).

[16]P. W. Lisowski, Ph.D. dissertation, Duke University, 1973.